



Cite this: *Chem. Sci.*, 2023, **14**, 566

All publication charges for this article have been paid for by the Royal Society of Chemistry

Received 28th September 2022
Accepted 27th November 2022

DOI: 10.1039/d2sc05413b

rsc.li/chemical-science

Introduction

With industrial applications encompassing heat-resistant adhesives, varnishes, UV coatings, textile finishing, and polymeric plastics,¹ (meth)acrylate esters are produced at the million-ton scale² and are considered to be among the most important manufactured chemicals. The desirable physical properties of poly(meth)acrylate esters, such as their flexibility, transparency, and weatherability, can also be controlled and fine-tuned to the requirements of their intended applications, most commonly *via* the functionalization of the ester group, which adds to their versatility.² While usually produced *via* the reaction of (meth)acryloyl chlorides with alcohols, the production of functionalized (meth)acrylates through a transesterification process^{3–7} instead would theoretically reduce the amount of stoichiometric halide wastes produced. The use of methyl (meth)acrylates (MA and MMA) instead of their corresponding carboxylic acids is also advantageous in terms of handling given their superior solubility profiles in organic solvents.

^aGraduate School of Engineering, Nagoya University, B2-3(611) Furo-cho, Chikusa, Nagoya 464-8603, Japan. E-mail: ishihara@cc.nagoya-u.ac.jp

^bSection of Theoretical Catalytic Chemistry, Institute for Catalysis, Hokkaido University, Sapporo, Hokkaido 011-0021, Japan. E-mail: hasegawa@cat.hokudai.ac.jp

^cVenture Business Laboratory, Nagoya University, B2-4 Furo-cho, Chikusa, Nagoya 464-0814, Japan

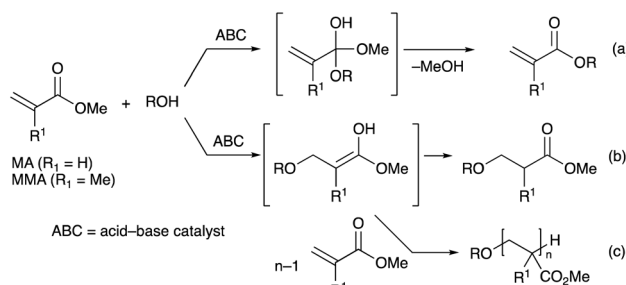
† Electronic supplementary information (ESI) available. CCDC 2152692 and 2151275. For ESI and crystallographic data in CIF or other electronic format see DOI: <https://doi.org/10.1039/d2sc05413b>

Bulky magnesium(II) and sodium(I) bisphenoxide catalysts for chemoselective transesterification of methyl (meth)acrylates†

Xue Zhao,^a Manussada Ratanasak,^b Kazumasa Kon,^{ac} Jun-ya Hasegawa^b and Kazuaki Ishihara^a

Given the industrial importance of (meth)acrylate esters, various groups have devoted considerable effort to investigating their chemoselective transesterification. In 2021, we developed magnesium(II) and sodium(I) complexes derived from 2,6-di-*tert*-butyl-*p*-cresol (BHT-H) as chemoselective catalysts for the transesterification of methyl acrylate (MA) and methyl methacrylate (MMA), respectively. Based on our results, we report the discovery of magnesium(II) and sodium(I) salts derived from 6,6'-(propane-2,2'-dyl) bis(2,4-di-*tert*-butylphenol) (PBTP-H₂), *i.e.* Mg(PBTP) and Na₂(PBTP), which are 41 and 81 times more effective catalysts than Mg(BHT)₂ and Na(BHT) for the transesterification of MA and MMA, respectively. These new catalysts are highly effective across an extensive range of alcohols, including primary and secondary alcohols, diols, and triols. Overall, this efficient transesterification technology can be expected to find practical applications in industrial process chemistry.

(Meth)acrylate esters are α,β -unsaturated esters capable of undergoing both Michael addition⁸ and transesterification.^{3–7} The extent of each of the two competing pathways depends on the character of the nucleophile and the mode of activation of the carbonyl group: nucleophiles with higher charge density, also known as “hard” nucleophiles, and carbonyl groups activated by a densely charged Lewis acid, such as that of a metal cation, tend to undergo nucleophilic substitution (Scheme 1a), whereas Michael addition is favored by “soft” nucleophiles that have better molecular orbital matching with the carbon–carbon double bond (Scheme 1b).⁹ As a result, a competent catalytic system for the transesterification of (meth)acrylate esters must exhibit excellent chemoselectivity toward the nucleophilic substitution reaction to maximize the transesterification



Transesterification (a):

favoured by hard nucleophiles and Lewis-acid activation of ester group

Michael addition (b) and polymerization (c):

favoured by soft nucleophiles or radical species and minimal/no activation of ester group

Scheme 1 Nucleophilic reactions of alcohols to MA or MMA.



product yield. This is especially difficult in the case of MA, which has the least sterically hindered α,β -unsaturated end in comparison to other acrylate analogues, and is therefore more prone to undergo the undesired Michael addition reaction. In fact, the harsh reaction conditions employed in many acid/base-related transesterification strategies invariably cause not only undesirable Michael addition reactions, but also the premature Michael-addition-initiated polymerization of MA or MMA (Scheme 1c), which results in low monomeric product yield.

Given the industrial significance of (meth)acrylates, it is hardly surprising that various groups have devoted considerable effort to the investigation of their chemoselective transesterification. In line with the aforementioned Lewis-acid activation strategy to favor transesterification, much attention has been paid to the application of heterogenous metal catalysts such as Ti(v),¹⁰ Zr(iv),¹¹ and Ca(NO₃)₂/ γ -Al₂O₃,¹² to chemoselective transesterifications. However, the main concerns in all the afore-mentioned studies are the physical and catalytic properties of the heterogenous catalysts; the substrate scopes of the systems are underdeveloped and remains unexplored. It is unclear whether these catalysts can efficiently catalyze the transesterification of acrylates with other structurally distinct alcohols, such as complex primary alcohols, secondary alcohols, and diols.

In 2016, Ohshima accomplished the chemoselective transesterification of MMA and MA with a diverse array of primary alcohols, diols, and triols with excellent yield and selectivity using a zinc(ii) cluster catalyst,⁶ albeit that examples of secondary alcohols were lacking.^{6h} It should also be noted here that 20 mol% of toxic 4-(dimethylamino)pyridine (DMAP) is required as a ligand for this catalytic system to function optimally, which poses severe environmental concerns for its widespread adoption as a viable industrial solution. Thus, in 2017, Hashimoto and Ootsuka at Toagosei Co., Ltd. reported a new catalytic method using triethylenediamine (DABCO) and zinc(acrylate).⁶ⁱ According to the patent,⁶ⁱ Michael addition of DABCO to MMA gives an enolate anion, which is further transformed to a dimeric vinyl ester intermediate through transesterification with MMA. Subsequently the transesterification of this intermediate with primary alcohol occurs to give the corresponding ester and MMA.

In 2018, we developed tetramethylammonium methyl carbonate as an efficient, general and metal-free catalyst for transesterification reactions.^{5b} This catalyst has been successfully applied across a wide range of ester and alcohol partners, including examples using MMA as a substrate in reactions with secondary alcohols, diols, and triols; however, reactions using MA give complex mixtures.

It was evident that the chemical research community had made great headway in the development of catalysts capable of the efficient and chemoselective transesterification of (meth)acrylate esters. Nonetheless, a truly robust, economical, and environmentally friendly catalytic system capable of this feat remained elusive and warranted further research.

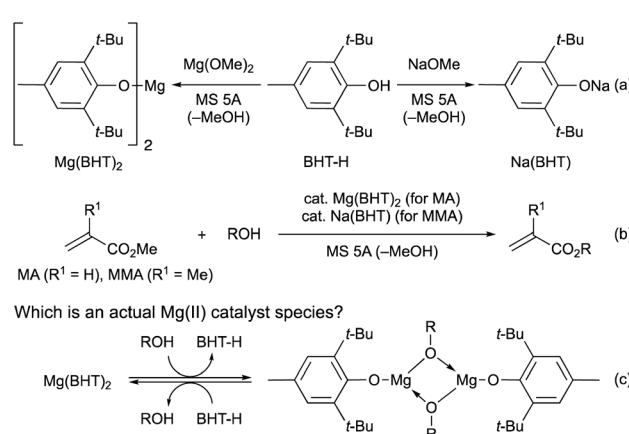
In 2021, we developed magnesium(ii) and sodium(i) complexes (Mg(BHT)₂ and Na(BHT)) derived from 2,6-di-*tert*-butyl-*p*-cresol (BHT-H) as efficient and chemoselective catalysts

for the transesterification of MA and MMA, respectively (Schemes 2a and b).⁷ These catalysts are effective for various primary and secondary alcohols, diols, triols, and even tetraols. Interestingly, dimeric Mg(ii) complexes, [Mg(OAr)(OR)]₂, have been proposed as active species in the ring-opening polymerization (ROP) reactions.¹³ Therefore, we considered a mechanistic possibility including such dimeric Mg(ii) complexes based on DFT calculations (Scheme 2c) in our previous paper.⁷ The observed energy profiles showed that [Mg(OAr)(OR)]₂ favors the transesterification pathway over the Michael-addition pathway. Additionally, according to the DFT results, the dimeric Mg(ii) complex (R = Bn) is by only 1.0 kcal mol⁻¹ more stable than the monomeric Mg(ii) complex.

Based on our previous study,⁷ we report herein the discovery of magnesium(ii) and sodium(i) salts derived from 6,6'-(propane-2,2'-diyl)bis(2,4-di-*tert*-butylphenol) (PBTP-H₂), *i.e.*, Mg(PBTP) and Na₂(PBTP), which serve as new catalysts for the transesterification of MA and MMA, respectively (Scheme 3). These catalysts are easily prepared from inexpensive chemicals, are much more active than Mg(BHT)₂ and Na(BHT),⁷ and are effective across an extensive range of alcohols including primary and secondary alcohols as well as diols and triols. In general, this efficient transesterification technology can be expected to be attractive for practical applications in the context of industrial process chemistry.

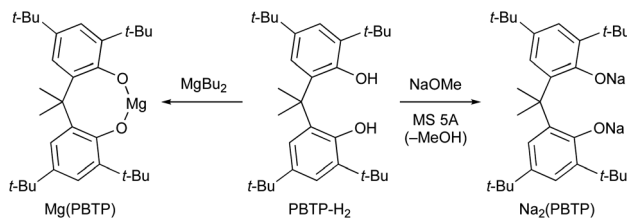
Results and discussion

Initially, the chemoselectivity of several magnesium(ii) aryl-oxides for the transesterification of MA with benzyl alcohol (1a) was estimated under equilibrium conditions without MS 5A. Representative results are shown in Table 1. When the *in situ*-generated Mg(BHT)₂ was used as the catalyst, the desired product (2a) was obtained in 40% yield together with side product 6a (1% yield) from the competing Michael addition after 30 minutes (entry 1). Much to our delight, Mg(PBTP) was able to furnish 2a in 55% yield after 1 hour without any formation of undesirable side products (entry 2).



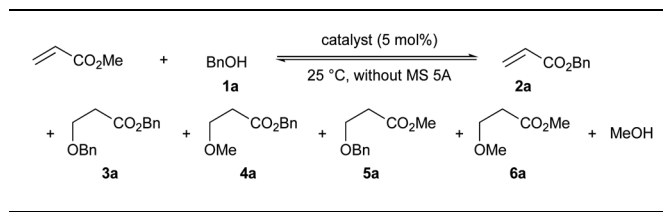
Scheme 2 Transesterifications of MA and MMA catalyzed by Mg(BHT)₂ and Na(BHT), respectively.





Scheme 3 This work: new catalysts for chemoselective transesterification of MA and MMA.

Table 1 Comparison of the chemoselectivity of catalysts for the transesterification of MA with **1a** under equilibrium conditions^a



Entry	Catalyst	Yield [%] of 2a/3a/4a/5a/6a ^b		
		0.5 h	1.0 h	3.0 h
1 ^c	Mg(BHT) ₂	40/0/0/0/1	—	70/0/0/1/4
2	Mg(PBTP)	41/0/0/0/0	55/0/0/0/0	—
3	Bu ₂ Mg	57/0/2/2/0	67/1/4/3/0	—

^a Unless otherwise noted, the reaction was carried out using MA (14 mmol), **1a** (2 mmol), catalyst (5 mol%), Cu(CS₂NMe₂)₂ (polymerization inhibitor, 0.2 mol%), and MS 5A (0.4 g) at 25 °C. ^b The yield was determined via ¹H NMR analysis using dimethylsulfone as an internal standard. ^c Previous data from ref. 7.

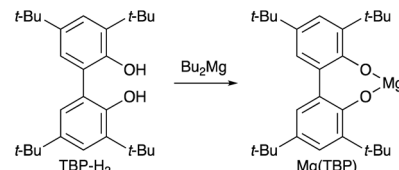
Dibutylmagnesium also showed high catalytic activity, but exhibited a low level of chemoselectivity (entry 3). Side products **3a** (1% yield), **4a** (4% yield), and **5a** (3% yield) were detected together with the formation of the desired product **2a** (67% yield).

Next, we attempted the transesterification of MA with isoborneol (**1b**) as a model reaction using magnesium(II) aryloxides as catalysts, and monitored the reaction progress at various time intervals to compare their catalytic activity. The respective results are summarized in Table 2. We first tried Mg(BHT)₂, and after 6, 8, and 12 hours, **2b** was detected in 62%, 85%, and 91% yield, respectively; after 19 hours, **2b** was obtained in 99% yield (entry 1). The use of Mg(PBTP) provided **2b** in 90% and 99% yield after 6 and 8 hours, respectively (entry 2). A comparison of entry 1 with entry 2 suggests that the bidentate ligation of Mg(PBTP) plays an important role in increasing the catalytic activity. Based on this inspired discovery, we then examined Mg(TBP), which was generated *in situ* from Bu₂Mg and 3,3',5,5'-*tert*-butyl-1,1'-biiphenyl-2,2'-diol (TBP-H₂). However, only 35% and 42% yields of **2b** were detected after 6 and 8 hours, respectively; after 24 hours the yield of **2b** reached just 60% (entry 3). Interestingly, the ring size of the metalacyclic structure, in addition to the bidentate ligation of the magnesium(II) aryloxides, is also important for increasing the catalytic activity.

Table 2 Comparison of catalytic activities for the transesterification of MA with **1b**^a

Entry	Catalyst	Yield [%] of 2b ^b				
		6 h	8 h	12 h	19 h	24 h
1	Mg(BHT) ₂	62	85	91	99	—
2	Mg(PBTP)	90	99	—	—	—
3	Mg (TBP) ^c	35	42	—	—	60

^a Unless otherwise noted, the reaction was carried out using MA (14 mmol), **1b** (2 mmol), catalyst (5 mol%), Cu(CS₂NMe₂)₂ (polymerization inhibitor, 0.2 mol%), and MS 5A (0.4 g) at 25 °C. ^b The yield was determined via ¹H NMR analysis using dimethylsulfone as an internal standard. ^c TBP-H₂ and Mg (TBP) are shown as follows.



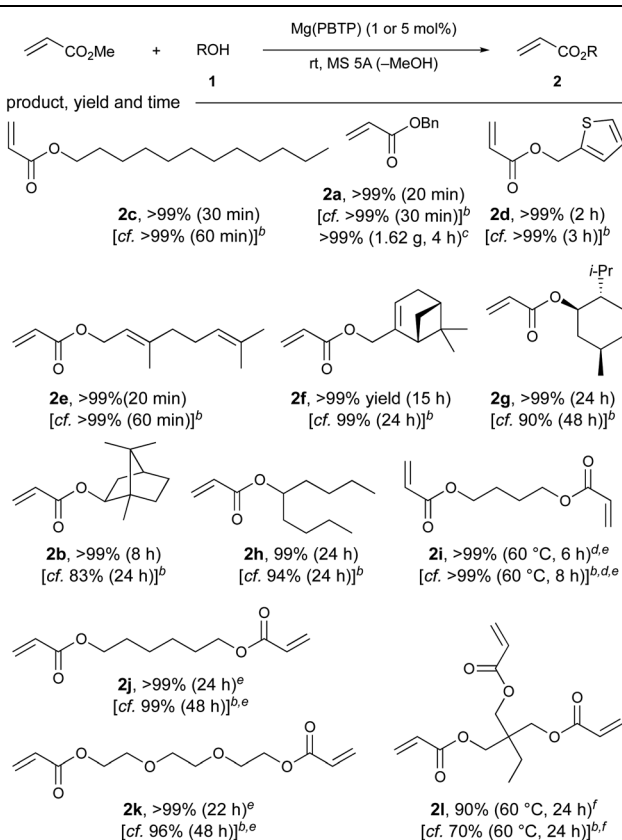
Next, the substrate scope of Mg(PBTP) as a catalyst for the transesterification of MA was investigated as shown in Table 3. Mg(PBTP) was more active than Mg(BHT)₂, and the transesterification was completed much faster. The transesterification proceeded with primary alcohols such as a saturated fatty alcohol (**1c**), allylic alcohols (**1e**, **1f**), and (hetero)arylmethyl alcohols (**1a**, **1d**) to give the desired esters in quantitative yield. We were able to scale up the test reaction by a factor of five to obtain 1.62 g of **2a** (>99% yield, 4 h) using a lowered catalytic load of 1 mol% Mg(PBTP), demonstrating the viability of the catalytic system for the gram-scale synthesis.

Additionally, Mg(PBTP) was applicable to secondary alcohols, although longer reaction times were required. For example, (−)-menthyl acrylate (**2g**), which is potentially useful for the synthesis of pressure-sensitive adhesives (PSA),¹⁴ and isoborneol-derived acrylate **2b** were obtained in >99% yield. 5-Nonanyl acrylate (**2h**), a monomer for synthesis that is a common additive for UV-adhesives, was also synthesized successfully.¹⁵

Trimethylolpropane acrylate **2l**, which is commonly used in the production of UV coatings and has also recently found applications in the development of superswelling hydrogels¹⁶ and as an alumina pigment modifier,^{5c} was successfully obtained in 90% yield after 24 hours. This result represents a successful chemoselective transesterification of an industrially useful triol. We increased the amount of 5A molecular sieves to 800 mg to account for the three-fold increase in equivalents of the side product methanol produced per molecule of target product. The transesterification of various



Table 3 Substrate scope of Mg(PBTP) as a catalyst for the transesterification of MA^a

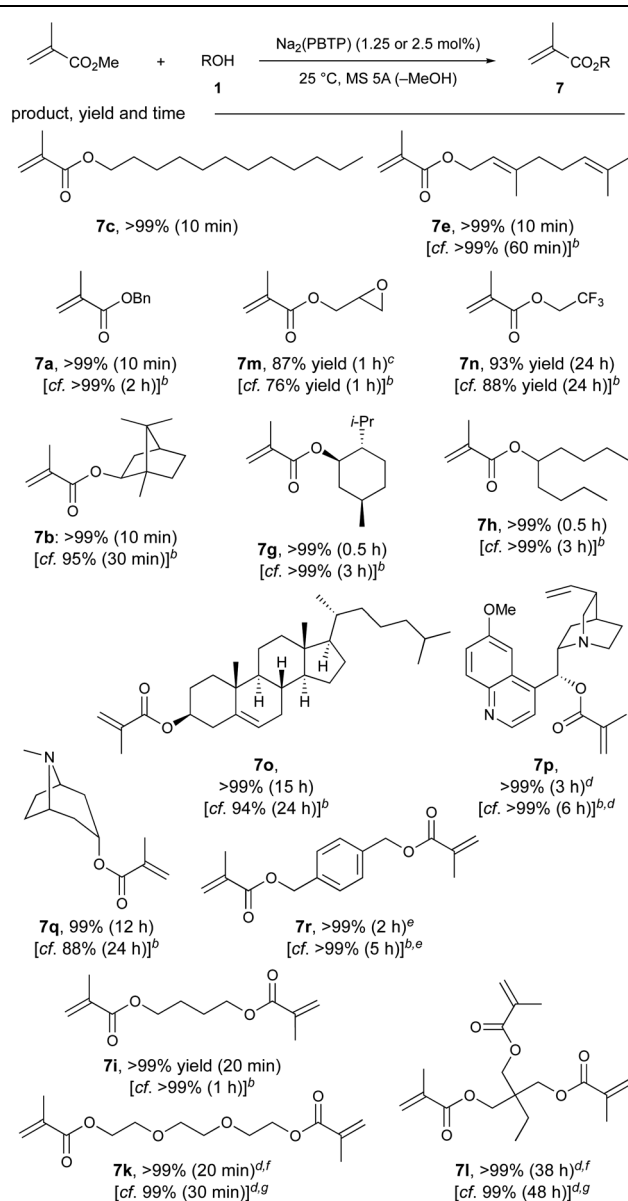


^a Unless otherwise noted, the reaction was carried out using MA (14 mmol), **1** (2 mmol), Mg(PBTP) (5 mol%), Cu(CS₂NMe₂)₂ (polymerization inhibitor, 0.2 mol%), and MS 5A (0.4 g) at 25 °C. Isolated yields after flash column chromatography on silica gel are shown. ^b Mg(BHT)₂ was used instead of Mg(PBTP) under otherwise identical conditions. See ref. 7. ^c The reaction was carried out using MA (70 mmol), **1a** (10 mmol), Mg(PBTP) (1 mol%), Cu(CS₂NMe₂)₂ (polymerization inhibitor, 0.2 mol%), and MS 5A (2 g) at 25 °C. ^d Mg(PBTP) (10 mol%) was used. ^e MS 5A (0.6 g) was used. ^f MS 5A (0.8 g) was used.

industrially useful diols (**1i–1k**) to produce **2i–2k** was also successful with extraordinary yields (>99%) and reaction times of 6–24 hours. Once again, we used a higher amount of 5 Å molecular sieves (600 mg) for these diols to facilitate the removal of methanol.

Next, we focused on the chemoselective transesterification of MMA. As expected, Mg(PBTP), as well as Mg(BHT)₂, were less effective for MMA. Fortunately, Na₂(PBTP) (1.25 mol%) was highly effective and superior to Na(BHT) (2.5 mol%), as shown in Table 4. Under the standard reaction conditions, all the primary alcohols (**1c**, **1e**, **1a**) gave the corresponding products in quantitative yield within 10 minutes. Glycidyl methacrylate (**7m**), which is chelating and particularly susceptible to nucleophilic attack, which sometimes results in its decomposition and polymerization, was obtained in 87% yield.^{5b–d} Trifluoroethyl methacrylate (**7n**), which is also unstable due to its electron-withdrawing nature was also obtained in 93% yield.¹⁷

Table 4 Substrate scope of Na₂(PBTP) as a catalyst for the transesterification of MMA^a



^a Unless otherwise noted, the reaction was carried out with MMA (14 mmol), **1** (2 mmol), Na₂(PBTP) (1.25 mol%), 4-acetamido-TEMPO (polymerization inhibitor, 0.1 mol%), and MS 5A (0.4 g) at 25 °C. Isolated yields after flash column chromatography on silica gel are shown. ^b Na(BHT) (2.5 mol%) was used instead of Na₂(PBTP) (1.25 mol%) under otherwise identical conditions. See ref. 7. ^c MS 5A (0.8 g) was used. ^d MMA (28 mmol) and MS 5A (0.8 g) were used. ^e MS 5A (0.6 g) was used. ^f Na₂(PBTP) (2.5 mol%) was used. ^g Na(BHT) (5 mol%) was used.

Quinine methacrylate (**7p**), a potentially useful monomer for the synthesis of molecularly imprinted polymers for the screening of halides and amino acids,¹⁸ was successfully obtained in quantitative yield despite its notable steric demand. Similarly, other *sec*-alkyl methacrylates such as **7b**, **7g**, **7h**, and **7o** were successfully synthesized. The efficacy of Na₂(PBTP) was



highlighted by the facile transesterification of diols to furnish diesters **7r**, **7i**, and **7k** quantitatively in a shorter time. In addition to these successful results, transesterification of trimethylolpropane (**1l**) quantitatively furnished triester **7l** when an increased catalyst loading of $\text{Na}_2(\text{PBTP})$ (2.5 mol%) was used.

Finally, we turned our attention to the mechanistic aspects. The molecular structures of $\text{Mg}(\text{PBTP})$ and $\text{Na}_2(\text{PBTP})$ were determined *via* single-crystal X-ray diffraction analysis (Fig. 1). Interestingly, $\text{Mg}(\text{PBTP})$ was crystallized in THF as the dimeric complex $[\text{Mg}(\text{PBTP}) \cdot \text{THF}]_2$. On the other hand, $\text{Na}_2(\text{PBTP})$ was crystallized in THF as the monomeric complex $\text{Na}_2(\text{PBTP}) \cdot 4(\text{THF})$, which was stabilized through a double sodium(*i*)- η^6 -benzene structure. Under the transesterification conditions, MA, MMA, and **1** coordinative to $[\text{Mg}(\text{PBTP})]_2$ and $\text{Na}_2(\text{PBTP})$ to replace the THF molecules.

To numerically verify the higher catalytic activity of $\text{Mg}(\text{PBTP})$ compared to that of $\text{Mg}(\text{BHT})_2$, density functional theory (DFT) calculations were performed for the transesterification of MA with **1a** catalyzed by $[\text{Mg}(\text{PBTP})]_2$ based on its crystal structure shown in Fig. 1.¹⁹ The potential energy profile is explained in Fig. 2 and 3. The pathway shown is the most plausible in the present study. $[\text{Mg}(\text{PBTP})]_2$ is stabilized by the coordination of **1a**. **1a** is then activated as **Int1** by intramolecular proton transfer in $[\text{Mg}(\text{PBTP})]_2 \cdot \text{1a}$ *via* **TS1**. In addition, MA is also activated as **Int2** by coordination of **Int1**. Nucleophilic addition of BnO^- to MA in **Int2** then occurs *via* **TS2** to form **Int3**. This is the rate-determining step (RDS), and the calculated activation energy is $10.8 \text{ kcal mol}^{-1}$ (E_{a2}^{EDS}). Thus, this elementary step includes both proton transfer from **1a** to OAr and C–O formation in a stepwise manner. Subsequently,

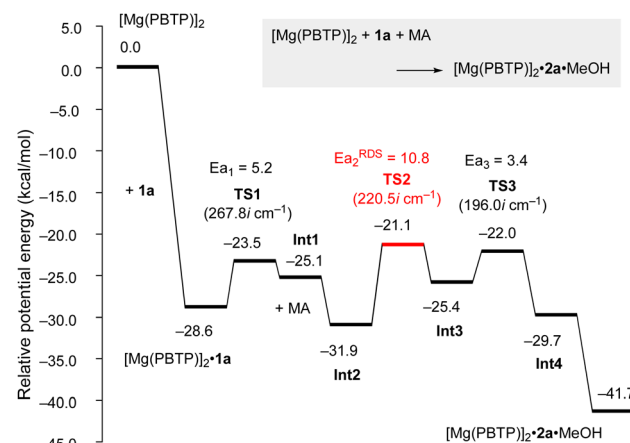


Fig. 2 Potential energy profile for the transesterification of MA with **1a** using $[\text{Mg}(\text{PBTP})]_2$. Energies are given in kcal mol^{-1} . For transition states, imaginary frequencies are given in parentheses. For computational details, see ref. 19.

methanol is released from **Int3** *via* **TS3**. As shown in Table 5, the E_{a2}^{EDS} value using $[\text{Mg}(\text{PBTP})]_2$ is $2.2\text{--}5.2 \text{ kcal mol}^{-1}$ lower than those using $\text{Mg}(\text{PBTP})$, $\text{Mg}(\text{BHT})_2$, and $[\text{Mg}(\text{BHT})(\text{OBn})]_2$. In particular, the E_a^{EDS} difference ($2.2 \text{ kcal mol}^{-1}$) between $[\text{Mg}(\text{PBTP})]_2$ and $[\text{Mg}(\text{BHT})(\text{OBn})]_2$ enhances the rate constant of RDS for the former, which is by a factor of 41 higher than that of the latter.²⁰ This estimation provides a reasonable interpretation for the experimental activity enhancement of $[\text{Mg}(\text{PBTP})]_2$ as shown in Table 3.

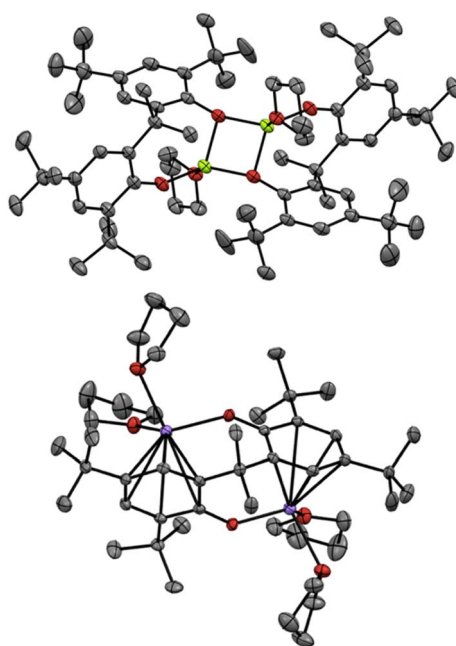


Fig. 1 Molecular structures of $[\text{Mg}(\text{PBTP}) \cdot \text{THF}]_2$ (top) and $\text{Na}_2(\text{PBTP}) \cdot 4(\text{THF})$ (bottom) with thermal displacement ellipsoids at 50% probability; Hydrogen atoms are omitted for clarity.

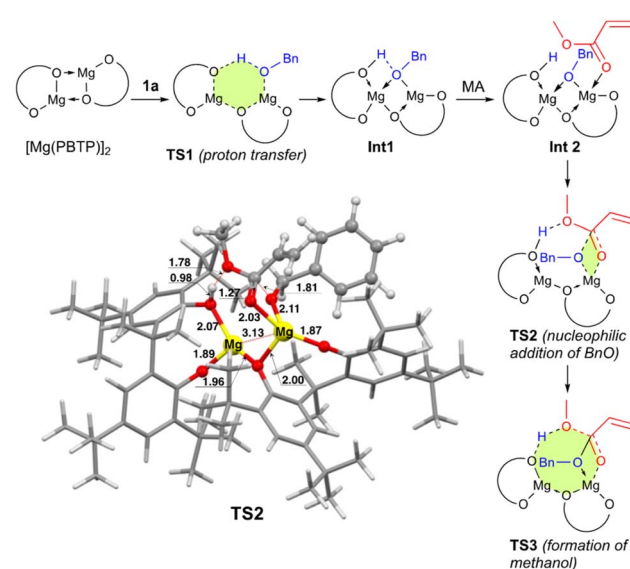


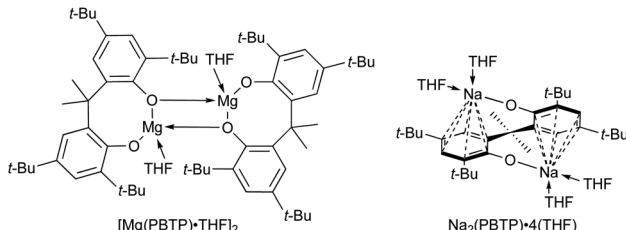
Fig. 3 Optimized structure of **TS2**. Bond lengths are given in \AA . Selected transition state and intermediate structures based on Fig. 2 are also shown. For computational details, see ref. 19.



Table 5 Comparison of the activation energy for the rate determining step^a

Catalyst	E_a^{RDS} [kcal mol ⁻¹]	Catalyst	E_a^{RDS} [kcal mol ⁻¹]
$\text{Mg}(\text{BHT})_2^{\text{b},\text{c}}$	14.9	$\text{Mg}(\text{PBTP})^{\text{b}}$	16.0
$[\text{Mg}(\text{BHT})(\text{OBn})]_2^{\text{b},\text{c}}$	13.0	$[\text{Mg}(\text{PBTP})]_2^{\text{b}}$	10.8
$\text{Na}(\text{BHT})^{\text{c},\text{d}}$	21.4	$\text{Na}_2(\text{PBTP})^{\text{d}}$	18.8

^a For computational details, see ref. 19. ^b Calculated for the transesterification of MA with **1a**. ^c See ref. 7. ^d Calculated for transesterification of MMA with **1a**.



Next, DFT calculations were performed for the transesterification of MMA with **1a** catalyzed by $\text{Na}_2(\text{PBTP})$ based on its crystal structure shown in Fig. 1. In this case, **1a** and MMA are activated at the same time by coordination of $\text{Na}_2(\text{PBTP})$. Subsequently both proton transfer from **1a** to OAr and nucleophilic addition of BnO^- occur *via* **TS4** to give **Int5** in a concerted manner. This is the RDS, and the calculated activation energy is 18.8 kcal mol⁻¹ (E_a^{RDS}). As shown in Table 5, the E_a^{RDS} value using $\text{Na}_2(\text{PBTP})$ is 2.6 kcal mol⁻¹ lower than that using $\text{Na}(\text{BHT})$. This difference in E_a^{RDS} enhances the rate constant of RDS for $\text{Na}_2(\text{PBTP})$, which is by a factor of 81 higher than that for $\text{Na}(\text{BHT})$.²⁰

This estimation provides a reasonable interpretation for the experimental activity enhancement of $\text{Na}_2(\text{PBTP})$ shown in Table 4.

Since $\text{Na}_2(\text{PBTP})$ has two Na sites, another possibility is sequential transesterification at the other Na site. This indicates one Na site has MMA and **1a** and ready for the reaction. The other Na site is coordinated by the product of the reaction. In fact, this structure corresponds to **Int5** in Fig. 4. The **Int5** state is 15.4 kcal mol⁻¹ higher than the reactant state, $\text{Na}_2(\text{PBTP})\cdot 2(\text{MMA})\cdot 2(\mathbf{1a})$. This result indicates that **7a** and MeOH are predominantly produced from **Int5**, MMA, and **1a**, and $\text{Na}_2(\text{PBTP})\cdot 2(\text{MMA})\cdot 2(\mathbf{1a})$ is regenerated at the same time. Thus, the possibility of the sequential transesterification at the other Na site of **Int5** is ruled out.

Conclusions

In summary, we have developed the catalysts $[\text{Mg}(\text{PBTP})]_2$ and $\text{Na}_2(\text{PBTP})$, which are highly effective for the chemoselective transesterification of MA and MMA, respectively, under mild conditions at 25 °C. These catalysts are superior to $\text{Mg}(\text{BHT})_2$ and $\text{Na}(\text{BHT})$, respectively, which we had previously developed.⁷ The results of DFT calculations strongly support our experimental results. Overall, based on the observed chemoselectivity, high yields, mild conditions, and lack of toxic metal species, the catalytic methods reported here represent new practical, green, and sustainable catalyst candidates for the industrial synthesis of acrylates.

Data availability

The data supporting this study is available within the main text and the associated ESI.†

Author contributions

K. I. conceived and directed the project. X. Z. and K. K. carried out the experiments and collected data. M. R. performed and analyzed the DFT calculations under the supervision of J. H. K. I. wrote the manuscript with contributions from all authors.

Conflicts of interest

There are no conflicts to declare.

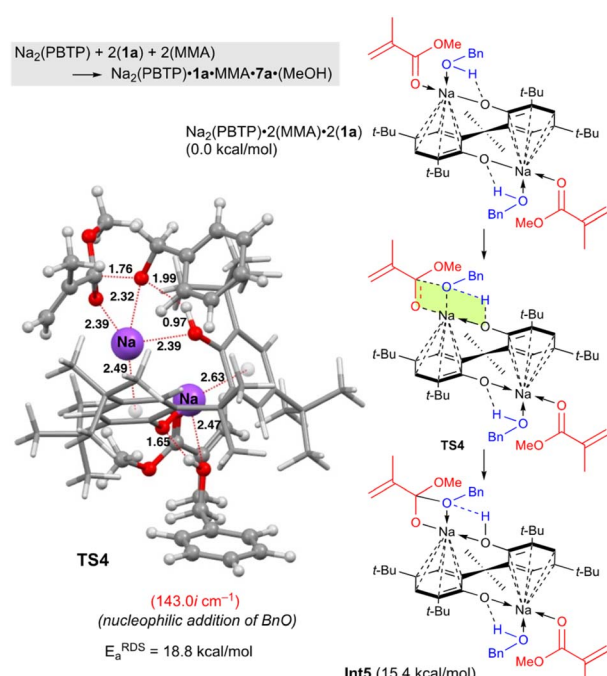


Fig. 4 Optimized structure of **TS4** for the transesterification of MMA with BnOH using $\text{Na}_2(\text{PBTP})$. Bond lengths are given in Å. Selected transition state and intermediate structures are also shown. For computational details, see ref. 19.



Acknowledgements

Financial support was partially provided by JSPS KAKENHI grants JP20K20559 (to K. I.) and JP20H02685 (to J. H.). K. I. is grateful for financial support from the Takahashi Industrial and Economic Research Foundation and the Nagoya University Research Fund. M. R. and J. H. are grateful for financial support from the Photo-excitonix Project at Hokkaido University and the Integrated Research Consortium on Chemical Sciences. This study was also supported by the Joint Usage/Research Center for Catalysis. Some of the computational calculations were carried out using the Research Center for Computational Science, Okazaki, Japan (Project: 22-IMS-C002). We thank Prof. Makoto Yamashita (Nagoya Univ.) and Mr Tao Ding (Nagoya Univ.) for their assistance with the X-ray diffraction analysis.

Notes and references

- (a) S. Thamizharasi and B. S. R. Reddy, *J. Appl. Polym. Sci.*, 2001, **80**, 1870–1879; (b) I.-L. Chien and K.-L. Zeng, *IFAC Proc. Vol.*, 2005, **38**, 141–146; (c) *Acrylic Acid, Acrylate Esters and Polymers - Chemical Economics Handbook (CEH) | IHS Markit*, <https://ihsmarkit.com/products/acrylic-acid-acrylate-esters-chemical-economics-handbook.html>, (accessed May 27, 2020).
- 2 A. Niesbach, H. Kuhlmann, T. Keller, P. Lutze and A. Górkak, *Chem. Eng. Sci.*, 2013, **100**, 360–372.
- 3 For reviews for catalytic transesterification, see: (a) J. Otera, *Chem. Rev.*, 1993, **93**, 1449–1470; (b) G. A. Grasa, R. Singh and S. P. Nolan, *Synthesis*, 2004, **36**, 971–985; (c) H. E. Hoydonckx, D. E. De Vos, S. A. Chavan and P. A. Jacobs, *Top. Catal.*, 2004, **27**, 83–96; (d) M. Hatano and K. Ishihara, *Chem. Commun.*, 2013, **49**, 1983–1997.
- 4 For La(III) catalysts for catalytic transesterification, see: (a) T. Okano, K. Miyamoto and J. Kiji, *Chem. Lett.*, 1995, **24**, 246; (b) A. A. Neverov and R. S. Brown, *Can. J. Chem.*, 2000, **78**, 1247–1250; (c) M. Hatano, Y. Furuya, T. Shimmura, K. Moriyama, S. Kamiya, T. Maki and K. Ishihara, *Org. Lett.*, 2011, **13**, 426–429; (d) M. Hatano, S. Kamiya, K. Moriyama and K. Ishihara, *Org. Lett.*, 2011, **13**, 430–433; (e) M. Hatano, S. Kamiya and K. Ishihara, *Chem. Commun.*, 2012, **48**, 9465–9467.
- 5 For onium salt catalysts for catalytic transesterification, see: (a) K. Ishihara, M. Niwa and Y. Kosugi, *Org. Lett.*, 2008, **10**, 2187–2190; (b) M. Hatano, Y. Tabata, Y. Yoshida, K. Toh, K. Yamashita, Y. Ogura and K. Ishihara, *Green Chem.*, 2018, **20**, 1193–1198; (c) S. Tanaka, T. Nakashima, T. Maeda, M. Ratanasak, J. Hasegawa, Y. Kon, M. Tamura and K. Sato, *ACS Catal.*, 2018, **8**, 1097–1103; (d) S. Tanaka, T. Nakashima, N. Satou, H. Oono, Y. Kon, M. Tamura and K. Sato, *Tetrahedron Lett.*, 2019, **60**, 2009–2013; (e) Y.-P. Lam, X. Wang, F. Tan, W.-H. Ng, Y.-L. S. Tse and Y.-Y. Yeung, *ACS Catal.*, 2019, **9**, 8083–8092.
- 6 For metal cluster catalysts for catalytic transesterification, see: (a) T. Ohshima, T. Iwasaki, Y. Maegawa, A. Yoshiyama and K. Mashima, *J. Am. Chem. Soc.*, 2008, **130**, 2944–2945; (b) T. Iwasaki, Y. Maegawa, Y. Hayashi, T. Ohshima and K. Mashima, *J. Org. Chem.*, 2008, **73**, 5147–5150; (c) T. Iwasaki, Y. Maegawa, Y. Hayashi, T. Ohshima and K. Mashima, *Synlett*, 2009, **20**, 1659–1663; (d) T. Iwasaki, K. Agura, Y. Maegawa, Y. Hayashi, T. Ohshima and K. Mashima, *Chem.-Eur. J.*, 2010, **16**, 11567–11571; (e) Y. Hayashi, T. Ohshima, Y. Fujii, Y. Matsushima and K. Mashima, *Catal. Sci. Technol.*, 2011, **1**, 230–233; (f) Y. Maegawa, T. Ohshima, Y. Hayashi, K. Agura, T. Iwasaki and K. Mashima, *ACS Catal.*, 2011, **1**, 1178–1182; (g) Y. Maegawa, K. Agura, Y. Hayashi, T. Ohshima and K. Mashima, *Synlett*, 2012, **23**, 137–141; (h) D. Nakatake, R. Yazaki and T. Ohshima, *Eur. J. Org. Chem.*, 2016, **2016**, 3696–3699; (i) N. Hashimoto and M. Ootsuka, *Jpn. Kokai Tokkyo Koho*, 2017, JP2017048172A; (j) H. Nagae, T. Hirai, D. Kato, S. Soma, S. Akebi, K. and K. Mashima, *Chem. Sci.*, 2019, **10**, 2860–2868.
- 7 J. Q. Ng, H. Arima, T. Mochizuki, K. Toh, K. Matsui, M. Ratanasak, J. Hasegawa, M. Hatano and K. Ishihara, *ACS Catal.*, 2021, **11**, 199–207.
- 8 P. B. Kisanga, P. Ilankumaran, B. M. Fetterly and J. G. Verkade, *J. Org. Chem.*, 2002, **67**, 3555–3560.
- 9 J. Clayden, N. Greeves, S. Warren and P. Wothers, *Organic Chemistry*, Oxford University Press, 2001.
- 10 For silica-supported Ti(IV) complexes, see: M. C. Gaudino, R. Valentin, D. Brunel, F. Fajula, F. Quignard and A. Riondel, *Appl. Catal. A*, 2005, **280**, 157–164.
- 11 For silica-supported Zr(IV) complexes, see: V. Salinier, G. P. Niccolai, V. Dufaud and J.-M. Basset, *Adv. Synth. Catal.*, 2009, **351**, 2168–2177.
- 12 M. Adriana, E. Nadine, C. Lorraine and F. François, *Appl. Catal. A*, 2013, **468**, 1–8.
- 13 I. E. Nifant'ev, A. V. Shlyakhtin, V. V. Bagrov, M. E. Minyaev, A. V. Churakov, S. G. Karchevsky, K. P. Birin and P. V. Ivchenko, *Dalton Trans.*, 2017, **46**, 12132–12146.
- 14 S.-S. Baek and S.-H. Hwang, *Eur. Polym. J.*, 2017, **92**, 97–104.
- 15 Osaka Organic Chemical Industry Ltd.: The leading company in acrylic acid esters, <http://www.ooc.co.jp/en/>, (accessed Jun 30, 2020).
- 16 E. Karadağ and D. Saraydin, *Polym. Bull.*, 2002, **48**, 299–307.
- 17 (a) A. Suzuki, M. Fujiwara and M. Nishijima, *Colloid Polym. Sci.*, 2008, **286**, 525–534; (b) F. Ziegert, M. Koof and J. Wagner, *Colloid Polym. Sci.*, 2017, **295**, 1563–1574.
- 18 (a) C.-G. Niu, A.-L. Guan, G.-M. Zeng, Y.-G. Liu, G.-H. Huang, P.-F. Gao and X.-Q. Gui, *Anal. Chim. Acta*, 2005, **547**, 221–228; (b) T. Ogawa, K. Hoshina, J. Haganaka, C. Honda, T. Tanimoto and T. Uchida, *J. Pharm. Sci.*, 2005, **94**, 353–362.
- 19 Computational details: Gaussian 16 (Rev. A.03); DFT method: ω B97xd/6-31G(d,p); solvent: PCM model using methyl propanoate as a solvent ($E_{\text{ps}} = 6.0777$). For more details, see Section 8 in the ESI.†
- 20 The Arrhenius equation ($T = 298$ K) was used, assuming that the pre-exponential factors for both complexes were identical.

